Gondo et al. International Journal of Mechanical and Materials Engineering (2018) 13:5
https://doi.org/10.1186/s40712-018-0091-0

International Journal of Mechanical and Materials Engineering

ORIGINAL PAPER Open Access

# Establishing a simple and reliable method of measuring ductility of fine metal wire

Shiori Gondo[1,2*], Shinsuke Suzuki[2,3], Motoo Asakawa[3], Kosuke Takemoto[4], Kenichi Tashima[4] and Satoshi Kajino[5]

## Abstract

**Background:** Measurement of the ductility like elongation and reduction of area of the fine metal wire is important because of the progress for the weight reduction and miniaturization of various products. This study established a simple and reliable method of measuring the ductility of a fine metal wire.

**Methods:** Tensile and loading-unloading tests were performed with applying initial load to high-carbon steel wire (diameters of 0.06–0.296 mm) through capstan-type grippers for non-metal fiber. The wire fastened with the grippers was separated into three parts: the fastened part, the contact part, and the non-contact part. Scanning electron microscope (SEM) images were used to measure the wire radius under uniform deformation and agreed well with the radius calculated using the radius before tensile testing and uniform elongation.

**Results:** The following conditions were clarified: non-slippage at the fastening between gripper and wire, a longitudinally uniform elongation, negligible cross-head bending, and the stroke calculation accuracy of elongated length by the initial load. Thus, uniform elongations were calculated as the ratio of the stroke at 0 N subtracted from the stroke at maximum tensile load to the additional initial chuck distance and the stroke at 0 N. The maximum error of uniform elongation was 0.21%. The reduction of area could be calculated by using the radius at uniform deformation portion, while the radius at the most constricted point was measured using SEM image of one fractured piece and uniform elongation. The measurement error of reduction of area was 1.9%.

**Conclusion:** This measurement method can be applied to other metal wires less than 1 mm in diameter.

**Keywords:** Fine metal wire, Tensile testing, Elongation, Reduction of area

## Background

Low-carbon steel wires, high-carbon steel wires, stainless steel wires, copper wires, aluminum wires, magnesium wires, gold wires, and amorphous wires have been used as materials for structures, medical devices, electrical devices, meshes, goods for hobby and so on (Yoshida 2000). These wires are required to be much finer than typical wires, because the weight reduction and miniaturization of various products has progressed. For example, gold wires less than 0.02 mm in diameter have been required because of decreasing spacing between bonding wires. Kim et al. investigated mechanical properties of ultra-fine Au wires for the development of a fine and high-strength Au wire (Kim et al. 2006). Daitoh et al. (Daitoh et al. 2000) and Tarui et al. (Tarui et al. 2005) developed the steel wire with a diameter of 0.02 mm and tensile strength higher than 4 GPa and investigated the microstructure of the wire. Furthermore, Li et al. succeeded in the development of ultra-fine steel wire with a diameter of 0.02 mm and tensile strength of 7 GPa (Li et al. 2014). However, ductility like an elongation of the wire was not measured sufficiently.

The applicable standard, International Organization for Standardization (ISO) 6892-1 (ISO 6982-1 2016), refers to a method for measuring the ductility of bulk metal using its elongation and reduction of area. In general, the elongation is measured from the extension of a wire. The extension is measured by an extensometer, not by the stroke increment of a cross-head (henceforth simply referred to as the stroke increment) which is measured by the rotation angle of a ball screw in a universal testing

* Correspondence: shiori-gondo78th@moegi.waseda.jp
[1]Graduate School of Fundamental Science and Engineering, Department of Applied Mechanics, Waseda University, Shinjuku, Tokyo 169-8555, Japan
[2]Kagami Memorial Research Institute of Materials Science and Technology, Waseda University, Shinjuku, Tokyo 169-0051, Japan
Full list of author information is available at the end of the article

machine. The stroke increment should be smaller than the genuine extension. This is because cross-heads bend during tensile testing due the application of a large tensile load to the wire. Therefore, the ISO standard recommends an extensometer be placed upon the tested wire. The reduction of area is calculated from the diameter of a wire prior to tensile testing, and the diameter at the most constricted point after tensile testing is complete. These diameters are measured by joining fractured pieces.

However, it is difficult to measure ductility of a fine wire in terms of handling based on ISO 6892-1. For a wire with a diameter less than 0.2 mm, an elaborate measurement method for elongation has traditionally been required, even though the elongations and reductions of area of the wires greater than 0.2 mm in diameter have been calculated successfully (Ochiai et al. 1993; Zelin 2002; Hyung et al. 2007). For example, Khatibi et al. used a non-contact extensometer to perform tensile testing on a wire with a diameter under 0.1 mm (Khatibi et al. 2004). However, using such non-contact extensometers is a time-consuming process. Furthermore, the authors have measured the reduction of area in a wire with a 0.06-mm diameter using scanning electron microscope (SEM) images of a fractured piece following tensile testing. It is necessary to discuss the difference of reduction of area occurred by drawing conditions is not measurement error but significant difference (Gondo et al. 2015, 2016). An accuracy of the measurement method for reduction of area is required to be verified in detail again.

For a fine wire, it is necessary to use tensile testing tools and a load cell with a small capacity because such fine wires will only sustain small tensile loads. Capstan-type grippers are conventionally recommended for gripping non-metal fibers (JIS R3420 2013) but can be applied to a fine metal wire even though the tensile strength of these fine wires is 6.3–7.0 GPa and is much greater than the strength of non-metal fibers (Li et al. 2012, 2014). Additionally, the amount of cross-head bending during tensile testing might be negligible in these situations. Thus, the stroke increment can be regarded as the wire extension. This investigation focused on a tensile testing method of fastening the wire to the grippers under an initial load, as it is difficult to prevent the wire from slackening without an initial force. In this case, the wire is elastically deformed, such that the genuine initial length is shorter than the superficial length. The genuine initial length, the stroke at 0 N, must therefore be calculated. The stroke at 0 N can be extrapolated using the slope of the stroke-tensile testing force. To apply this method, the validity of capstan-type gripper use must be verified, including the following conditions: no slip at the fastening between the gripper and wire, and longitudinally uniform elongation. Furthermore, the validity of regarding the stroke increment as the extension of the wire should be considered with the following conditions: negligible cross-head bending and stroke calculation accuracy at 0 N from the slope of the stroke increment and test force-stroke curve. If the validity of using capstan-type grippers and regarding the stroke increment as the wire extension are verified, it is possible to draw the nominal stress-nominal strain curve and calculate elongation. The accuracy of the elongation calculated using the stroke can be determined by comparing this value to the elongation calculated using an extensometer.

The production of the cross-sectional area and the longitudinal length of a wire remains constant during tensile testing until a maximum tensile load is applied to the wire. As such, the reduction of area can be calculated with the radius of the wire at uniform deformation portion, the radius of the most constricted point, and the uniform elongation. The radius of the wire at the uniform deformation portion and the most constricted point can be measured using SEM images of a fractured piece after tensile testing is complete. Before applying this, though, the validity of the calculation method for reduction of area using SEM images of a fractured piece must be established.

Given the requirements set forth in the above section, the purpose of this study was to establish a simple and reliable method of measuring the ductility of a fine metal wire. The following points are discussed: the validity of using capstan-type grippers, the validity of regarding the stroke increment as the extension of the wire, the accuracy of calculating the elongation using stroke increment, and the validity of the reduction of area calculation method using SEM images of a fractured piece of wire. The correspondence between experimental and examined items is shown in Table 1.

## Methods

### Starting materials

The starting materials were patented pearlitic steel wires with diameter of 0.444 mm and 0.98% carbon, provided by Nippon Steel & Sumikin SG Wire Co., Ltd. The chemical compositions of the wires, as shown in Table 2, were measured based on Japanese Industrial Standards (JIS) G1211-3 (JIS G1211-3 2011), G1212 (JIS G1212 1997), and G1258 (JIS G1258-3 2014). These refer to the quantitative analysis of C, Si, and other relevant elements, respectively.

### Wire drawing

A wet-type non-slip wire drawing machine was used in this study (Factory Automation Electronics Inc., D3ULT-10D). A wire could be drawn continuously through five passes using this machine. The conditions for wire drawing are displayed in Table 3. The drawing strain for each individual pass was calculated as $2\ln(d_{n-1}/d_n)$, and the total drawing

**Table 1** Relationship between experimental and examined contents

| Experimental contents | | | Examined contents | | | | | |
|---|---|---|---|---|---|---|---|---|
| Measurement method | | Measurement items | Validity of using capstan-type grippers | | Validity of regarding the stroke increment as extension | | Accuracy of elongation | Validity of calculating $R_a$ with SEM image of fractured piece |
| | | | Non-slippage at fastened part | Uniformity of elongation | Non-bending | Range for slope | | |
| Tensile testing without extensometer | Height gauge | Slippage | ✓ | | | | | |
| | Loading weight | Friction force | | ✓ | | | | |
| | Dial gauge | Amount of bending | | | ✓ | | | |
| | Loading-unloading | Stroke at 0 N | | | | ✓ | | |
| | Chuck distance | Elongation | | ✓ | | | | |
| Tensile testing with extensometer | | Elongation | | ✓ | | | ✓ | |
| Observation through SEM | | Radius | | | | | | ✓ |

strain was calculated as 2ln ($d_0/d_{30}$). The symbol $d$ represents the diameter of the wire, and $n$ represents the pass number.

### Tensile test

Tensile testing without a video-type non-contact extensometer was performed at Waseda University. Tensile testing with the extensometer was performed at the Tokyo office of Shimadzu Co.

#### *Tensile testing without a video-type non-contact extensometer*

A load cell with a maximum range of 500 N was equipped on the lower side of a universal testing machine (Shimadzu Co., Autograph AG-25TB) cross-head. The upper gripper (Shimadzu Co., Pneumatic Capstan Grips for Yarn and Cables) was fixed to a joint connected to the load cell. The lower gripper was inserted at another joint that was fixed to the testing machine table. The distance between the lower edge of the upper gripper and the upper edge of the lower gripper was 50 mm in length, as shown in Fig. 1. It can thus be said that the length between point A and point B of the wire was 150 mm when the wire was fastened with an initial load. However, this length was not the genuine chuck distance because the wire was elastically deformed. A schematic of the tensile test is shown in Fig. 2, including a dial gauge, a height gauge, and pieces of gauge tape.

**Measurement of slippage at fastening between gripper and wire** Wires with diameters measuring either 0.063 or 0.296 mm were fastened to the upper gripper and the lower gripper and were pulled tight by the application of an initial load ranging from 0.5–3.0 N. Gauge tape (2 mm × 7 mm) was placed on the wire 10 mm from the fastened edge of the upper gripper, as shown in Fig. 2. A height gauge (Mitsutoyo Co., HD-AX) was fixed on the universal testing machine table. The positions of the fastened edge and the tape were measured prior to tensile testing. Next, the cross-head was elevated by 2 mm at a speed of 10 mm/min. The positions of the edge and the tape were again measured with the height gauge. The distance between the edge and the tape (upper gripper-tape gap) was calculated.

**Measurement of friction force at contact part between the gripper and the wire** A weight with a clip was equipped on one end of a wire (diameter 0.063 or 0.296 mm) for testing. For the 0.063-mm diameter wire, weights of 60, 120, and 150 g were used. These were 5, 10, and 20% of the maximum tensile load, respectively. A weight of 600 g was applied to the 0.296-mm diameter wire, 5% of the maximum tensile load. The other side of the wire was fastened by the lower gripper. The wire was laid over the upper gripper, as shown in Fig. 3. The cross-head was then elevated by 2 mm at a speed of 10 mm/min. A load cell was used to measure the testing force. The stroke increment was measured by the rotation angle of a ball screw in the universal testing machine.

**Table 2** Chemical compositions of steel wires (mass %)

| C | Si | Mn | P | S | Cr | Fe |
|---|---|---|---|---|---|---|
| 0.98 | 0.19 | 0.3 | 0.008 | 0.008 | 0.19 | Bal. |

**Table 3** Wire-drawing conditions

| Diameter [mm] | 0.444 | 0.296 | 0.217 | 0.137 | 0.093 | 0.063 | 0.042 |
|---|---|---|---|---|---|---|---|
| Pass number | 0 | 5 | 10 | 15 | 20 | 25 | 30 |
| Drawing strain for each individual pass | - | 0.156 | | | | | |
| Total drawing strain | 0 | 0.81 | 1.43 | 2.35 | 3.12 | 3.91 | 4.70 |
| Back stress [N] | 0 | 1.0 | 0.5 | 0.5 | 0.5 | 0.5 | 0.3 |
| Drawing speed [m/min] | - | 22 | 48 | 105 | 230 | 500 | 500 |

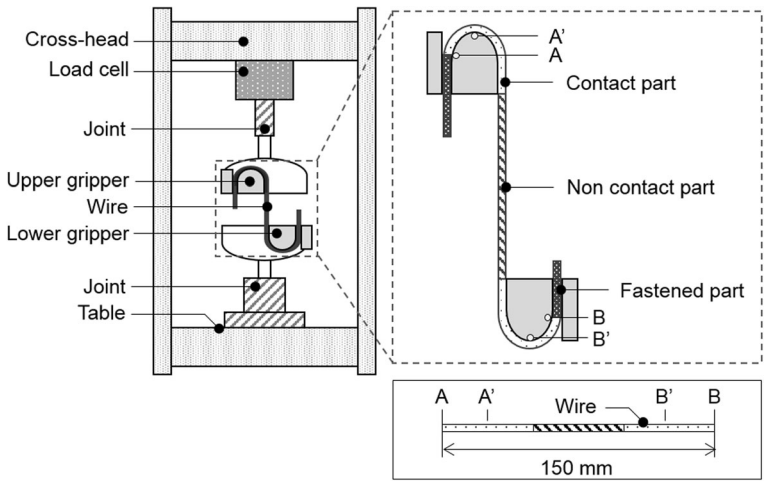


**Fig. 1** Schematic of tensile testing machine with a wire

**Measurement for cross-head bending in a universal testing machine** A dial gauge (Kyowa Electronic Instruments Co., Ltd., DT-30DM150) was set so that its pointer was located in front of a load cell in the horizontal center of a cross-head. The dial gauge and the universal testing machine were connected to a scanner (Kyowa Electronic Instruments Co., Ltd., USB-21A) and a data logger (Kyowa Electronic Instruments Co., Ltd., UCAM-20PC). In order to confirm that the pointer of the dial gauge remained parallel to the cross-head, steel sheet of 2.9 or 4.9 mm thick was inserted between the cross-head and the pointer. The thickness was then measured by the dial gauge. The thickness of the steel sheets was measured by a micrometer (Mitsutoyo Co., MDC-25MJ) beforehand. This verified that the difference in measurements was less than 0.1 mm. Thus, the parallelism of the pointer was confirmed. The cross-head was elevated by 5 mm at speed of 10 mm/min without a wire present. The stroke increment and the measured stroke, obtained using a dial gauge, were logged by the scanner and the data logger. Subsequently, a wire either 0.063 or 0.296 mm in diameter was fastened to the grippers with an initial load. Again, the cross-head was elevated 5 mm at speed of 10 mm/min. The stroke increment and the measured stroke obtained by the dial gauge were logged by the scanner and the data logger.

**Loading-unloading test** A wire of 0.063 or 0.296 mm in diameter was fastened to the grippers under an initial load. The cross-head was elevated by 0.25, 0.5, 0.75, and 1.0 mm before descending to a height of − 0.3 mm at speed of 10 mm/min. The testing force and the stroke increment were measured.

**Tensile test under various chuck distances** The cross-head was set at chuck distance of 150, 200, 300, 400, 500, or 600 mm. A wire of 0.063 or 0.296 mm in diameter was fastened to grippers under an initial load. The cross-

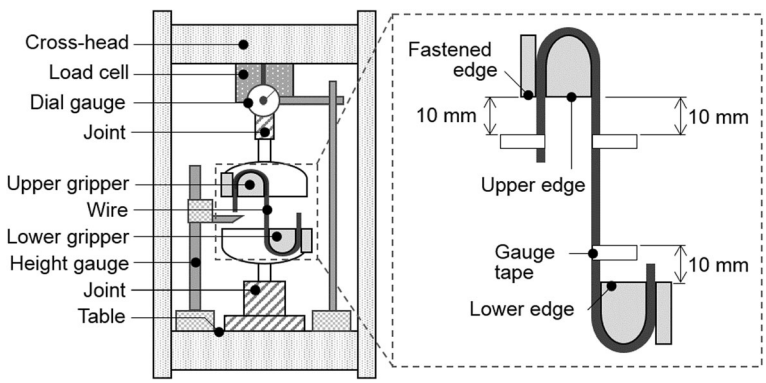


**Fig. 2** Schematic of tensile test with a dial gauge, a height gauge, and pieces of gauge tape

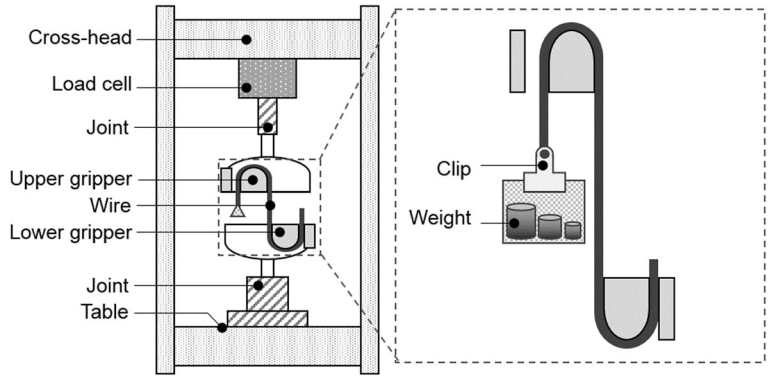


**Fig. 3** Schematic image of method of measuring friction force applied to the wire and the contact part of the upper gripper

head was elevated at a speed of 10 mm/min until the wire fractured. The testing force and the stroke increment were measured.

#### *Tensile test with a video-type non-contact extensometer*

A load cell with a maximum range of 1 kN was connected to the lower side of a universal testing machine cross-head (Shimadzu Co., Autograph AG-X-50kN). The grippers were fixed to the testing machine as described in the "Tensile testing without a video-type non-contact extensometer section." A video-type non-contact extensometer (Shimadzu Co., TRViewX 500D) was fixed to the front of the testing machine. A wire of 0.042, 0.063, 0.137, 0.216, or 0.296 mm in diameter was fastened to the grippers under an initial load. Two pieces of gauge tape were placed on the wire so that the gap between each tape and its nearest gripper was 10 mm, as shown in Fig. 2. The cross-head was elevated at a speed of 10 mm/min until the wire fractured. The distance between gauge tapes was measured by the extensometer.

### Observation of fractured piece

After tensile test, the wire was cut 15 mm away from its fractured point. A piece of carbon tape was put on the stage of an SEM (Hitachi Ltd., S2150). The cut wire was placed on the carbon tape so that the fractured point protruded 2–3 mm in from the edge of the tape. After observing the fractured piece, the sample stage was removed from the SEM. The wire was rotated 90° around its own axis. The sample stage was replaced in the SEM, and the fractured piece was again observed.

## Results and discussion

The relationship between the wire diameter and the increment of the upper gripper-tape gap is shown in Fig. 4. The slippage for the 0.063-mm diameter wire was almost 0. The error bar would show the measurement error caused by artificial reading error. For the 0.296-mm diameter wire, average slippage was 0.14 mm. So, the wire slipped slightly due to large tension of the fastened wire.

The relationship between the stroke increment and the testing force is shown in Fig. 5. At first, the testing force was seen to increase as the stroke increment increased. After this, the testing force became constant against the stroke increment. Further, increase in the testing force may result in a transition from a state of static friction to a kinetic friction state. On the other hand, a constant testing force might imply a state of kinetic friction. The kinetic friction force was calculated by subtracting the initial testing force from the testing force at the constant region mentioned above. The relationship between the weight and the kinetic friction force is shown in Fig. 6. The kinetic force was proportion to the weight. Therefore, the kinetic force can be measured using this method. The results shown in Fig. 5 can thus be considered appropriate.

The relationship between the stroke increment and the measured stroke obtained by a dial gauge without a

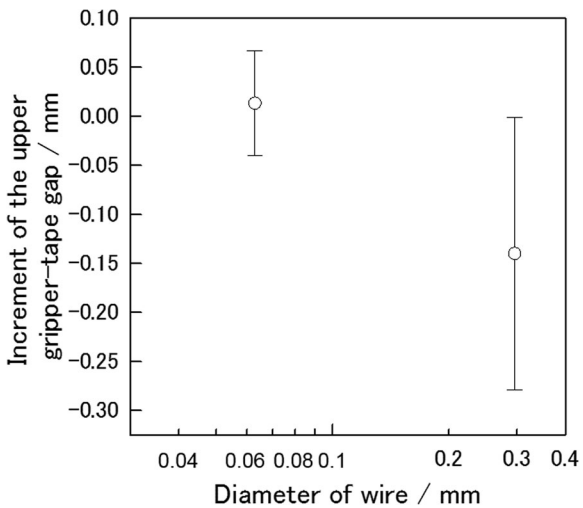


**Fig. 4** Relationship between the wire diameter and the increment of the upper gripper-tape gap

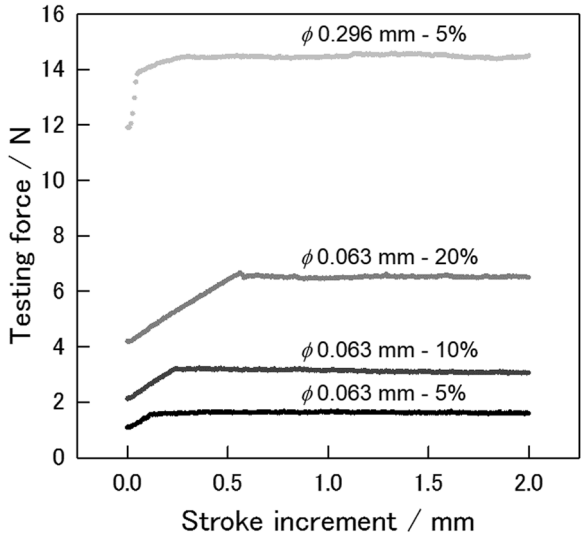


**Fig. 5** Relationship between the stroke increment and testing force. The weight with a clip was equipped on one end of a wire (diameter 0.063 or 0.296 mm) for testing. The weights were 5, 10, and 20% of the tensile load of the wire. The other side of the wire was fastened by the lower gripper

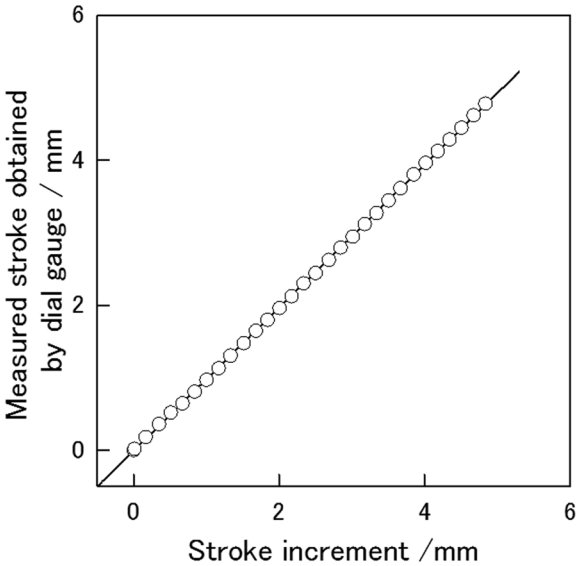


**Fig. 7** Relationship between the stroke increment and measured stroke obtained by a dial gauge without a wire

wire is shown in Fig. 7. The curve was approximated with a primary straight line through the origin. A similar test was performed with a wire. The relationship between the maximum tensile load of the wire and the slope of the straight line is shown in Fig. 8. The slope of the 0.063-mm diameter wire agreed well with the slope calculated without a wire. The slope for the 0.296-mm diameter wire was 0.02 smaller than that calculated without a wire. This value would correspond to a 0.01-mm difference if the cross-head was elevated by 5 mm. The amount of cross-head bending was 0.23% of elevated height of the cross-head. It can thus be stated that the amount of bending in the cross-head is negligible.

The stroke increment and testing force curve of (a) a 0.063-mm diameter wire and (b) a 0.296-mm diameter wire during loading and unloading are shown in Fig. 9. The slope of the curve during loading agreed with the slope during unloading for the wire of 0.063 mm diameter wire at all elevated heights under 1.0 mm. The

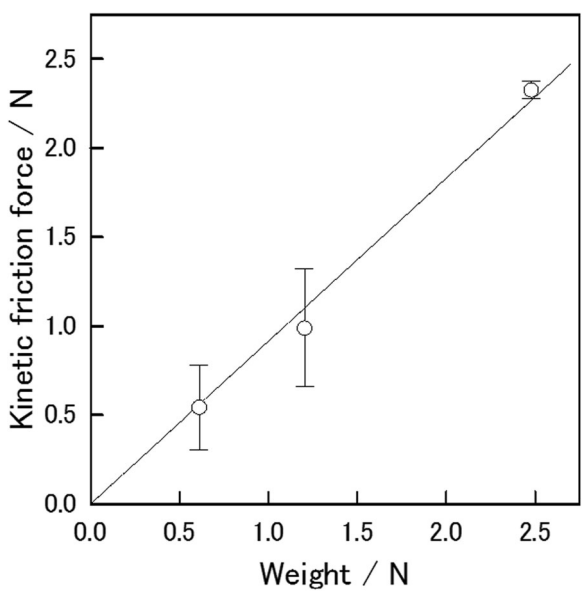


**Fig. 6** Relationship between the weight and the kinetic friction force

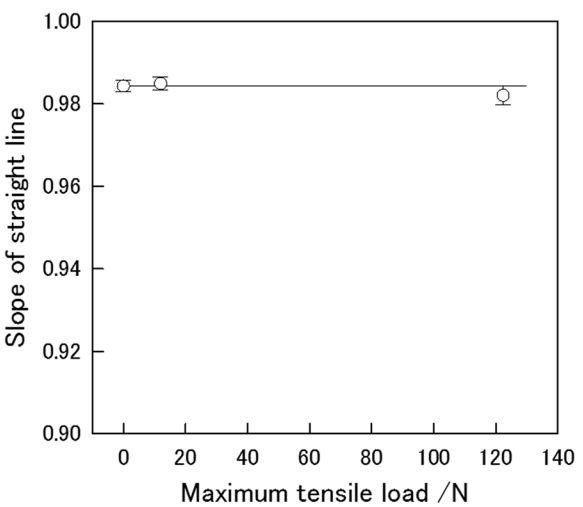


**Fig. 8** Relationship between maximum tensile load of the wire and the slope of the straight line. The plots at 12 and 122 N of the maximum tensile load are for wires of 0.063 and 0.296 mm diameter, respectively

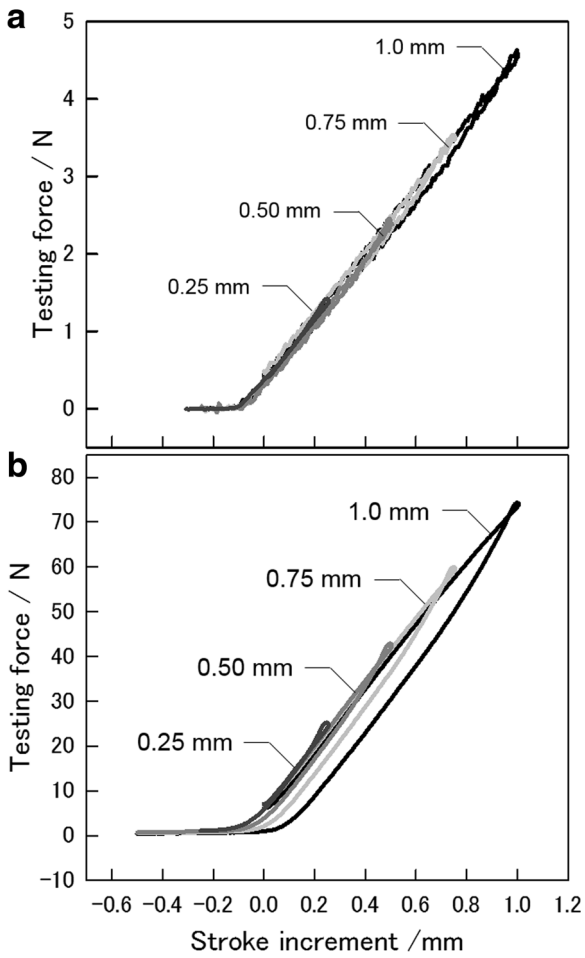


**Fig. 9** Stroke increment and testing force curve of the **a** 0.063- and **b** 0.296-mm diameter wire during loading and unloading. Elevated heights were 0.25, 0.50, 0.75, and 1.0 mm

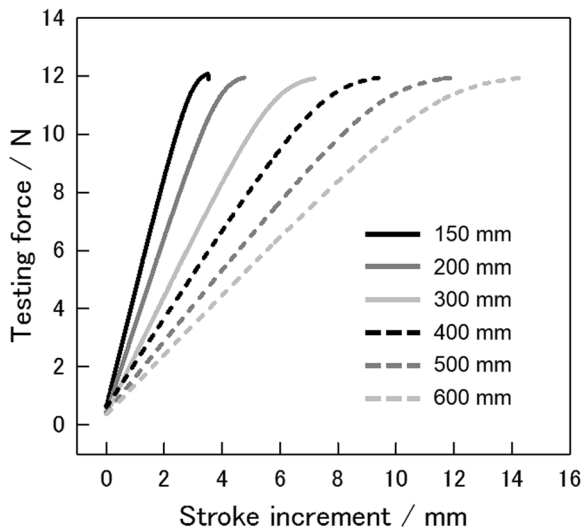


**Fig. 10** Stroke increment and testing force curve of the 0.063-mm diameter wire. Chuck distances were 150, 200, 300, 400, 500, and 600 mm in length

difference in slope caused by the elevated height was negligible. For the 0.296-mm diameter wire, the slope of the curve during loading was independent of the elevated height, and the slope observed during loading was different from the slope during unloading. Therefore, it was possible to calculate the slope in the stroke range from 0 to 1 mm. The stroke at 0 N, $u_0$, was calculated using the slope $a$ and the tensile load at 0 mm of stroke $F_0$, as stated in Eq. (1):

$$u_0 = -\frac{a}{F_0} \tag{1}$$

For the 0.063-mm diameter wire, the measured stroke at 0 N testing force was − 0.082 mm. The stroke calculated by extrapolation was − 0.087 mm. The maximum difference was 0.005 mm. Thus, the accuracy of this method of calculating the stroke at 0 N from the slope of the stroke increment and the testing force curve was verified. It should also be noted that the non-linearity of the curve during unloading at the elevated heights of 0.75 and 1.0 mm might be due to yielding of the wire during loading.

The stroke increment and testing force curve obtained for various initial chuck distances is shown in Fig. 10. The wire was fractured immediately after the maximum load was applied. The elongated lengths during local deformations were too small to measure. Therefore, the uniform elongation $e_{EL}$ was calculated. Thus, uniform elongation was calculated as shown in Eq. (2). The symbol $u_m$ represents the stroke at the maximum tensile load:

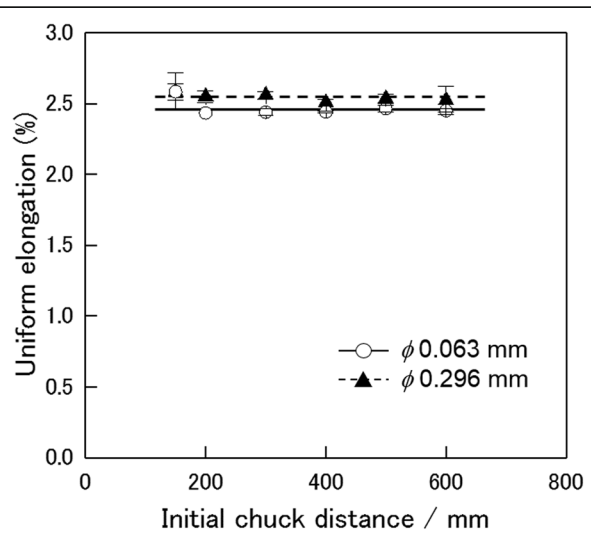


**Fig. 11** Relationship between chuck distance and uniform elongation of the 0.063- and 0.296-mm diameter wires

$$e_{\mathrm{EL}} = \frac{u_m - u_0}{150 + u_0} \times 100 \quad (2)$$

The relationship between the chuck distance and the uniform elongation is shown in Fig. 11. The difference in uniform elongation caused by chuck distance was not confirmed, even when the ratio of the contact part to the chuck distance decreased.

The relationship between the diameter of the wire and the uniform elongation calculated by the stroke increment and measured stroke obtained by the extensometer is shown in Fig. 12. With the exception of the 0.042-mm diameter wire, the difference in uniform elongations for each diameter wire was at most 0.21%. It can thus be stated that the uniform elongation calculated using the range over the contact part was highly similar to the one calculated using only the non-contact part. This implies the wire would be elongated uniformly at both its contact and non-contact parts (refer to Figs. 6, 11, and 12). The measurement error of uniform elongation caused by slippage was 0.37% for the 0.296-mm diameter, while the error was too small for the 0.063-mm diameter wire (refer to Fig. 4). Therefore, this measurement method is appropriate for the finer wire. Conversely, the difference in uniform elongations of the 0.042-mm diameter wire was large. The standard deviation obtained by the extensometer was also large. The stroke increment and testing force curve, the measured stroke obtained by the extensometer, and the testing force curve of the 0.042-mm diameter wire are shown in Fig. 13. It is clear from this figure that the stroke measured by the extensometer and the testing force curve were crooked. Image of the gauge tape tilt during tensile testing is shown in Fig. 14 at 0, 0.10, 0.41, and 0.74 mm of the stroke increment for the 0.042-mm diameter wire. In Fig. 14(a), the guide line of this wire was drawn at the wire, and white rectangles were drawn at the gauge tape to improve visibility. The crookedness seen in the curve is due to the tilt of the gauge tape during tensile testing.

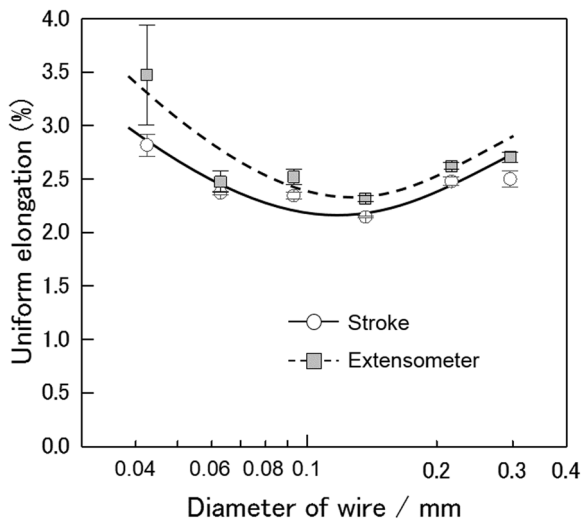


**Fig. 12** Relationship between the diameter of the wire and uniform elongation. Uniform elongation was calculated using a video-type non-contact extensometer and by cross-head stroke

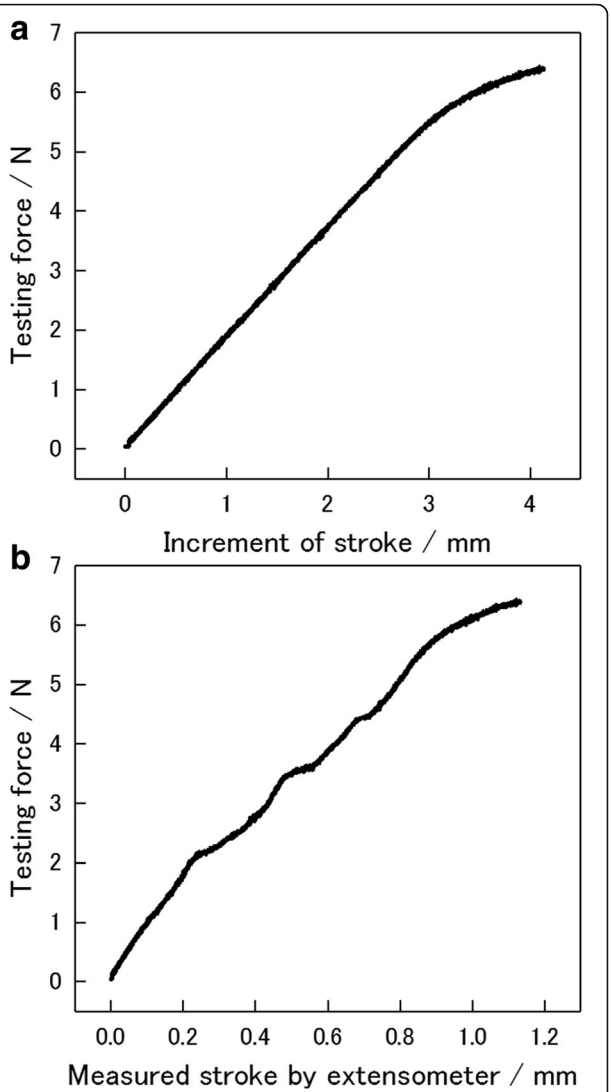


**Fig. 13 a** Stroke increment and testing force curve and **b** measured stroke obtained by extensometer-testing force curve of the 0.042-mm diameter wire

In the above paragraphs, the non-bending, non-slippage at fastened part, and uniformity of elongation conditions were verified, especially for the wire less than 0.1 mm. Furthermore, the validity of regarding the stroke increment as the extension was demonstrated. Therefore, a nominal stress and nominal strain curve could be drawn using the stroke, as shown in Fig. 15. The maximum nominal stress increased with decreasing diameter since work

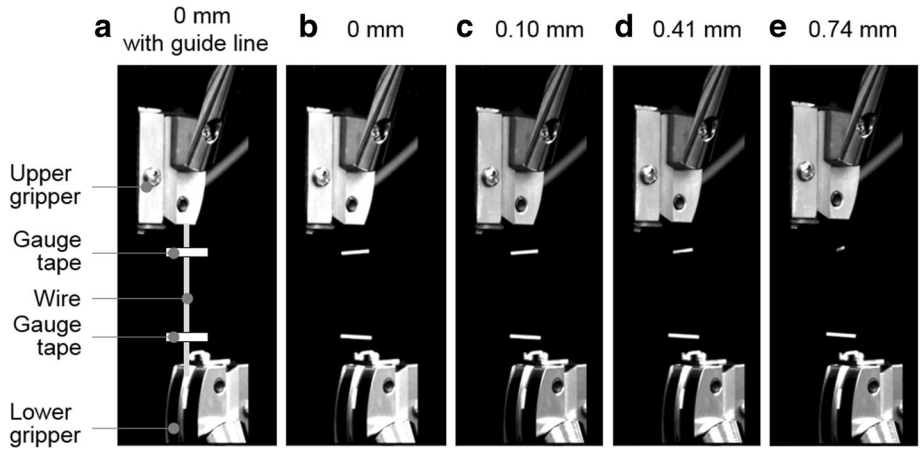


**Fig. 14** Image of the gauge tape tilts during tensile testing at **a** and **b** 0, **c** 0.10, **d** 0.41, and **e** 0.74 mm of the stroke increment for the 0.042 mm diameter wire. The guide line of the wire was drawn at the wire and white rectangles were drawn at the gauge tapes in order to improve visibility in **a**

hardening of the drawn wire. This tendency was similar to results reported by Zhang et al. (Zhang et al. 2011), Goto et al. (Goto et al. 2007), and Fang et al. (Fang et al. 2015). It can be said that not only the tensile strength but also the elongation will be measured well with regarding the stroke increment as extension of the wire.

Sample of SEM images of (a) the wire before tensile testing and (b) the fractured piece after tensile testing are shown in Fig. 16. A straight line $l_A$ was drawn along an outline of the wire on one side of the SEM image of the wire before tensile testing. The other straight line $l_B$ runs parallel to $l_A$ and was drawn along the outline on the other side. The straight center line $l_C$ was drawn directly between lines $l_A$ and $l_B$. The distance between line $l_C$ and the outer lines $l_A$ and $l_B$ was considered to be the radius of the wire $r_0$. Figure 16(b) shows the fractured piece has a constricted portion when compared to the SEM image of the wire before tensile testing. A straight line $l_D$ was drawn along the outline of the wire on one side of the SEM image of the fractured piece after tensile testing. The other straight line $l_E$ runs parallel to $l_D$ and was drawn along the wire outline on the other side. The range, the straight line fitted to the outline of the wire, can be considered to be the uniform deformation portion. The range, the straight line which did not fit the outline of the wire, can be considered to be the local deformation portion. The straight center line $l_F$ was drawn directly between $l_D$ and $l_E$. The distance between line $l_F$ and the outer lines $l_D$ and $l_E$ was considered to be the radius of the wire $r_1$. The straight line $l_G$ runs parallel to lines $l_D$,

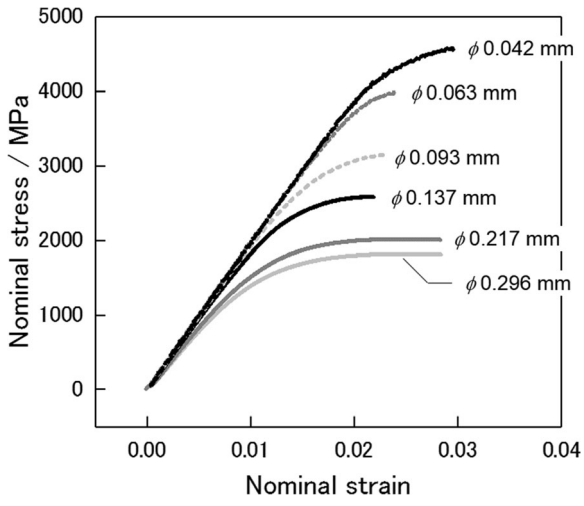


**Fig. 15** Nominal stress-nominal strain curve calculated by regarding the stroke increment as extension

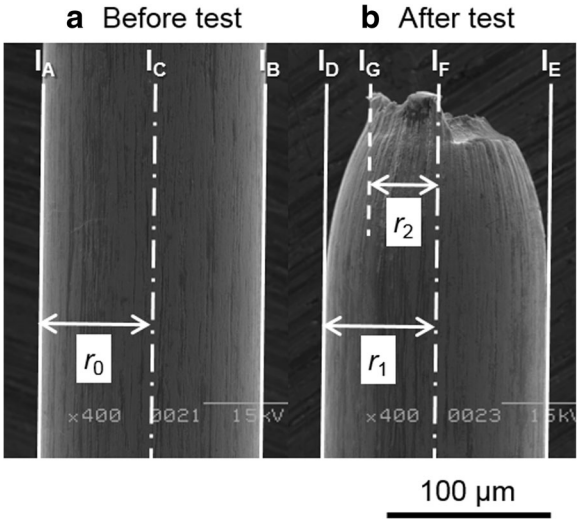


**Fig. 16** Sample SEM images of drawn wire before tensile testing and broken portion after tensile testing ($\varphi$ 0.137 mm)

$l_E$, and $l_F$ and was drawn at the most constricted point. The distance between lines $l_F$ and $l_G$ was considered to be the radius of the fractured wire at its most constricted point $r_2$. The wire deformed with constant volume until the maximum tensile load was applied to the wire. The ratio of the cross-sectional area of the wire before tensile testing to the cross-sectional area once the maximum tensile load had been applied to the wire had been calculated using uniform elongation with Eq. (3):

$$\left(\frac{\pi r_0}{\pi r_1}\right)^2 = 1 + \frac{e_{EL}}{100} \tag{3}$$

For the 0.063-mm diameter wire, the calculated ratio was 1.027 and the measured ratio was 1.024. For the 0.296-mm diameter wire, the calculated ratio was 1.029 and the measured ratio was 1.026. The difference between calculated and measured ratios is negligible. The deformation of the wire during tensile testing until maximum tensile load was applied to the wire could be supposed geometrically and theoretically verified. Therefore, the range of the straight line which fits the outline of the wire can be regarded as the uniform deformation portion. The range of the straight line which does not fit the outline of the wire can be regarded as the local deformation portion. The reduction of area can be calculated using the radius of the wire at the uniform deformation portion, the radius at the most constricted point and the uniform elongation using Eq. (4):

$$R_a = \left\{1 - \left(\frac{r_2}{r_1}\right)^2 \left(1 + \frac{e_{EL}}{100}\right)^{-1}\right\} \times 100 \tag{4}$$

The four reductions of area and the average of two 0.296-mm diameter wires, samples 1 and 2, are shown in Fig. 17. The averages were 67.1 and 62.7% for samples 1 and 2, respectively. The difference of averages was 4.4%. The standard deviations were 1.9 and 1.8 for samples 1 and 2, respectively. From above, the measurement error was at most 1.9%. The individual difference was 4.4%. Thus, reduction of area can be calculated with a 1.9% of measurement error. Since high-carbon steel wires have the highest tensile strength among metal wires, the amount of cross-head bending under high-carbon steel wire will be larger than that seen with other metal wires. Therefore, the measurement method presented in this study can be applied to the other metal wires under 1 mm in diameter. However, it is necessary to confirm two points for each too fine or fragile wire. The first is whether the wire can be fastened by grippers under an initial load. The second is whether testing forces can be increased with an increasing stroke increment while a cross-head is elevated without slippage.

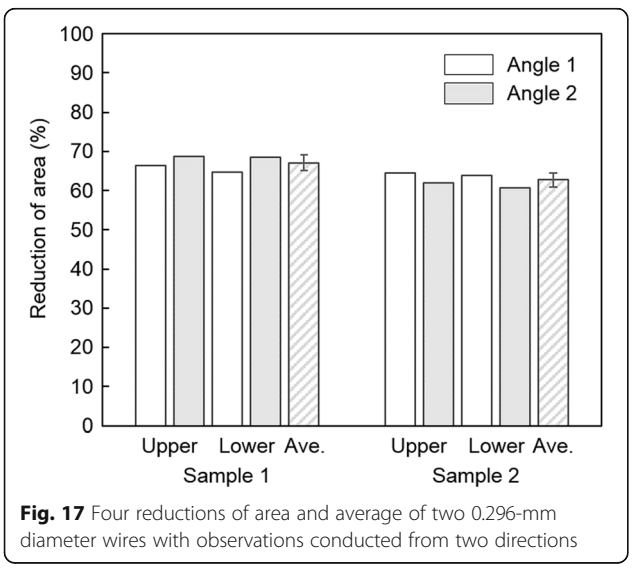


**Fig. 17** Four reductions of area and average of two 0.296-mm diameter wires with observations conducted from two directions

## Conclusions

Tensile testing of high-carbon steel wires less than 0.296 mm in diameter was performed by applying an initial load ranging from 0.5 to 3 N to the wire, and after testing, the fractured pieces were observed via SEM. The following conditions were then clarified: the validity of using capstan-type grippers, the validity of regarding the stroke increment as the extension of the wire, the accuracy of elongation calculated by the stroke, and the validity of the reduction of area calculation method using a SEM image of one fractured piece. From the above, a simple, reliable, and accurate measurement method for elongation and reduction of area were developed. These methods can be applied to other metal wires under 1 mm in diameter.

1. Elongation can be measured as the ratio of the stroke at 0 N subtracted from the stroke at the maximum tensile load to the additional initial chuck distance and the stroke at 0 N. The maximum error observed in the uniform elongation calculation was 0.21%. The stroke at 0 N testing force can be extrapolated using the slope of the stroke increment and the testing force curve. The stroke increment of a cross-head can be related to the extension of the wire. The slope can be calculated in the range of 0 to 1 mm stroke.
2. Reduction of area can be calculated using the radius of the wire at a uniform deformation portion, the radius at the most constricted point, and the uniform elongation. The measurement error was 1.9%. The radius of the wire at the uniform deformation portion can be measured by fitting straight lines to the wire outline on the SEM

image. The radius at the most constricted point can be also measured by fitting straight lines to the most constricted point.

## Nomenclature

$a$ Slope of stroke increment-tensile testing force curve
$d_n$ Diameter of the wire after the $n$th pass
$e_{EL}$ Uniform elongation
$F_0$ Tensile testing force at 0 mm of stroke
$n$ Pass number
$u_0$ Stroke at 0 N of tensile testing force
$u_m$ Stroke at maximum tensile load
$r_0$ Radius of the wire before tensile testing
$r_1$ Radius of the wire at uniform deformation portion after tensile testing
$r_2$ Radius of the wire at the most constricted point after tensile testing
$R_a$ Reduction of area

### Abbreviations
ISO: International Organization for Standardization; JIS: Japanese Industrial Standards; SEM: Scanning electron microscope

### Acknowledgements
This work was supported by JSPS Grant-in-Aid for JSPS Research Fellow Grant Number 16J11098 and was partly executed under the cooperation of organization between Waseda University and JXTG Nippon Oil & Energy Corporation. We would also like to express our gratitude to Nippon Steel & Sumikin SG Wire Co., Ltd. for giving materials and Shimadzu Corporation for permission to use a universal testing machine.

### Funding
The study received support from JSPS Grant-in-Aid for JSPS Research Fellow Grant Number 16J11098 and the cooperation of organization between Waseda University and JXTG Nippon Oil & Energy Corporation.

### Availability of data and materials
The datasets during and analyzed during the current study available from the corresponding author on reasonable request.

### Authors' contributions
SG designed the study; acquired, analyzed, and interpreted the data; and wrote the draft of the manuscript. SS contributed to designing the study and analysis and interpretation of the data and assisted in the preparation of the manuscript. All other authors helped design the study, interpret the data, and revise the manuscript. All authors approved the final version of the manuscript, and agreed to be accountable for all aspects of the work in ensuring that questions related to the accuracy or integrity of any part of the work are appropriately investigated and resolved.

### Authors' information
Gondo, S. is a Ph. D. course student at Waseda University.
Suzuki, S. is a professor at Waseda University.
Asakawa, M. is a Professor Emeritus at Waseda University.
Takemoto, K. is the CEO of Factory Automation Electronics Inc.
Tashima, K. is the Senior Vice President of Factory Automation Electronics Inc.
Kajino, S. is a senior researcher at National institute of Advanced Industrial Science and Technology.

## Publisher's Note


### Author details
[1]Graduate School of Fundamental Science and Engineering, Department of Applied Mechanics, Waseda University, Shinjuku, Tokyo 169-8555, Japan. [2]Kagami Memorial Research Institute of Materials Science and Technology, Waseda University, Shinjuku, Tokyo 169-0051, Japan. [3]Faculty of Science and Engineering, Department of Applied Mechanics and Aerospace Engineering, Waseda University, Shinjuku, Tokyo 169-8555, Japan. [4]Factory Automation Electronics Inc., Osaka, Osaka 533-0033, Japan. [5]National Institute of Advanced Industrial Science and Technology, Tsukuba, Ibaraki 305-8564, Japan.

Received: 5 November 2017 Accepted: 26 January 2018
Published online: 02 March 2018

### References
Daitoh, Y, Hamada, T. (2000). Microstructure of heavily-deformed high carbon steel wires. *Tetsu-to-Hagan*, *86-2*, 105–110.
Fang, F, Zhou, L, Hu, X, Zhou, X, Tu, Y, Xie, Z, Jiang, J. (2015). Microstructure and mechanical properties of cold-drawn pearlitic wires affect by inherited texture. *Materials and Design*, *79*, 60–67.
Gondo, S., Suzuki, S., Asakawa, M., Takemoto, K., Tashima, K., Kajino, S., (2015). Improvement of the limit of drawing a fine high carbon steel wire by decreasing back tension. Conference Proceedings for the 85th Annual Convention of the Wire Association International.
Gondo, S, Suzuki, S, Asakawa, M, Takemoto, K, Tashima, K, Kajino, S. (2016). Improvement of ductility with maintaining strength of drawn high carbon steel wire. *The Key Engineering Materials Journal*, *716*, 32–38.
Goto, S, Kirchheim, R, Al-Kassab, T, Borchers, C. (2007). Application of cold drawn lamellar microstructure for developing ultra-high strength wires. *Transactions of Nonferrous Metals Society of China*, *17*, 1129–1138.
Hyung, R, Eui, G, Won, J. (2007). Effect of alloying elements on work hardening behavior in cold drawn hyper-eutectoid steel wires. *Materials Science and Engineering A*, *449-451*, 1147–1150.
ISO 6982-1:2016. Metallic materials—tensile testing—part1: method of test at room temperature.
JIS G1211-3. (2011). Iron and steel—determination of carbon content - Part 3: Infrared absorption method after combustion.
JIS G1212. (1997). Iron and steel—methods for determination of silicon content-.
JIS G1258-3. (2014). Iron and steel—ICP atomic emission spectrometric method - Part 3; Determination of various elements- Decomposition with acids and fusion with sodium carbonate.
JIS R3420. (2013). Testing methods for textile glass products.
Khatibi, G, Stickler, R, Gröger, V, Weiss, B. (2004). Tensile properties of thin Cu-wires with a bamboo microstructure. *Journal of Alloys and Compounds*, *378*, 326–328.
Kim, KS, Song, JY, Chung, EK, Park, JK, Hong, SH. (2006). Relationship between mechanical properties and microstructure of ultra-fine gold bonding wires. *Mechanics of Materials*, *38*, 119–127.
Li, Y, Choi, P, Goto, S, Borchers, C, Raabe, C, Kirchheim, R. (2012). Evolution of strength and microstructure during annealing of heavily cold-drawn 6.3 GPa hypereutectoid pearlitic steel wire. *Acta Materialia*, *60*, 4005–4016.
Li, Y, Raabe, D, Herbig, M, Choi, P, Goto, S, Kostka, A, Yarita, H. (2014). Segregation stabilizes nanocrystalline bulk steel with near theoretical strength. *Physical Review Letters*, *113*, 106104.
Ochiai, I, Nishida, S, Tahiro, H. (1993). Effect of metallurgical factors of strengthening of steel tire cord. *Wire Journal International*, *12*, 50–61.
Tarui, T, Maruyama, N, Tshiro, H. (2005). Cementite decomposition in high carbon steel wires. *Tetsu-to-Hagan*, *91-2*, 265–271.
Yoshida, K. (2000). FEM analysis of wire breaks in drawing of superfine wire with an inclusion. *Wire Journal International*, *3*, 102–107.
Zelin, M. (2002). Microstructure evolution in pearlitic steels during wire drawing. *Acta Materialia*, *50*, 4431–4447.
Zhang, X, Godfrey, A, Huang, X, Hansen, N, Liu, Q. (2011). Microstructure and strengthening mechanism in cold-drawn pearlitic steel wire. *Acta Materialis*, *59*, 3422–3430.